Biochem. J. (1988) 250, 761–772 (Printed in Great Britain)

Consequences of molecular recognition in the S_1–S_2 intersubsite region of papain for catalytic-site chemistry

Change in pH-dependence characteristics and generation of an inverse solvent kinetic isotope effect by introduction of a P_1–P_2 amide bond into a two-protonic-state reactivity probe

Keith BROCKLEHURST,* Devanand KOWLESSUR,* Geeta PATEL,*§ William TEMPLETON,* Kim QUIGLEY,† Emrys W. THOMAS,‡ Christopher W. WHARTON,† Frances WILLENBROCK*‖ and Ron J. SZAWELSKI†

*Department of Biochemistry, St. Bartholomew's Hospital Medical College, University of London, Charterhouse Square, London EC1M 6BQ, U.K., †Department of Biochemistry, University of Birmingham, PO Box 363, Birmingham B15 2TT, U.K., and ‡Department of Biological Sciences, University of Salford, Salford M5 4WT, U.K.

1. The pH-dependences of the second-order rate constant (k) for the reactions of papain (EC 3.4.22.2) with 2-(acetamido)ethyl 2′-pyridyl disulphide and with ethyl 2-pyridyl disulphide and of k for the reaction of benzimidazol-2-ylmethanethiol (as a minimal model of cysteine proteinase catalytic sites) with the former disulphide were determined in aqueous buffers at 25 °C at I 0.1. 2. Of these three pH–k profiles only that for the reaction of papain with 2-(acetamido)ethyl 2′-pyridyl disulphide has a rate maximum at pH approx. 6; the others each have a rate minimum in this pH region and a rate maximum at pH 4, which is characteristic of reactions of papain with other 2-pyridyl disulphides that do not contain a P_1–P_2 amide bond in the non-pyridyl part of the molecule. 3. The marked change in the form of the pH–k profile consequent upon introduction of a P_1–P_2 amide bond into the probe molecule for the reaction with papain but not for that with the minimal catalytic-site model is interpreted in terms of the induction by binding of the probe in the S_1–S_2 intersubsite region of the enzyme of a transition-state geometry in which nucleophilic attack by the $-S^-$ component of the catalytic site is assisted by association of the imidazolium ion component with the leaving group. 4. The greater definition of the rate maximum in the pH–k profile for the reaction of papain with an analogous 2-pyridyl disulphide reactivity probe containing both a P_1–P_2 amide bond and a potential occupant for the S_2 subsite {2-(*N*′-acetyl-L-phenylalanylamino)ethyl 2′-pyridyl disulphide [Brocklehurst, Kowlessur, O'Driscoll, Patel, Quenby, Salih, Templeton, Thomas & Willenbrock (1987) Biochem. J. **244**, 173–181]} suggests that a P_2–S_2 interaction substantially increases the population of transition states for the imidazolium ion-assisted reaction. 5. The overall kinetic solvent ^2H-isotope effect at pL 6.0 was determined to be: for the reaction of papain with 2,2′-dipyridyl disulphide, 0.96 (i.e. no kinetic isotope effect), for its reaction with the probe containing only the P_1–P_2 amide bond, 0.75, for its reaction with the probe containing both the P_1–P_2 amide bond and the occupant for the S_2 subsite, 0.61, and for $k_{cat.}/K_m$ for its catalysis of the hydrolysis of *N*-methoxycarbonylglycine 4-nitrophenyl ester, 0.67. 6. The development of a rate maximum at pH approx. 6 appears to correlate in these reactions of papain with the development of an inverse kinetic solvent isotope effect ($k^{^1H_2O}/k^{^2H_2O} < 1$). Possible interpretation of these data and of data for other reactions of papain in the literature is discussed in terms of breaking of a hydrogen bond within the $-S^- \cdots H\text{-}Im^+-$ ion-pair. Ethyl 2-pyridyl disulphide was prepared by reaction of pyridine-2-thione with ethyl ethanethiolsulphonate; the pK_a of its conjugate acid was determined by spectral analysis at 310 nm to be 2.9, and that for the conjugate acid of 2-(acetamido)ethyl 2′-pyridyl disulphide was similarly determined to be 2.5.

INTRODUCTION

Papain (EC 3.4.22.2) (reviewed by Lowe, 1976; Brocklehurst *et al.*, 1981; Polgár & Halász, 1982; Kamphuis *et al.*, 1985*b*; Baker & Drenth, 1987; Brocklehurst, 1987; Brocklehurst *et al.*, 1988) is the most thoroughly studied of the cysteine proteinases. Its crystal structure has been refined to a resolution of 0.165 nm (Kamphuis *et al.*, 1984), and it provides valuable opportunities to investigate the coupling of binding-site interactions with catalytic-site chemistry (Brocklehurst, 1986; Brocklehurst *et al.*, 1987), which appears to be an important part of the molecular recognition process for this enzyme.

The interaction of proteinases with oligopeptide substrates and inhibitors is now generally discussed in terms of the P–S notation introduced by Schechter & Berger (1967, 1968) (see Berger & Schechter, 1970) in connection with their studies on papain, with due regard for the continuum of flexibility in the extended binding areas of the enzymes (Fruton, 1977, 1982) and of the consequences of this for variation and degree of fit in the

§ Present address: Department of Surgery, St. George's Hospital Medical School, Cranmer Terrace, London SW17 0RE, U.K.
‖ Present address: Department of Biochemistry, University of Oxford, South Parks Road, Oxford OX1 3QU, U.K.

assumed P–S complementarities. Major features of the specificity requirements of papain for substrates and inhibitors deduced from substrate-cleavage patterns, crystallographic and steady-state kinetic studies and model building (Schechter & Berger, 1967, 1968; Berger & Schechter, 1970; Wolthers *et al.*, 1970; Lowe & Yuthavong, 1971*a*; Lowe, 1976; Drenth *et al.*, 1976) are for a hydrophobic side chain at P_2 and the presence of a P_1–P_2 amide bond. The principal feature of the catalytic site of papain is a nucleophilic interactive system involving the side chains of Cys-25 and His-159, whose existence is detected particularly convincingly by using small 2-pyridyl disulphides as two-protonic-state reactivity probes (Brocklehurst, 1974, 1982). The problem involved in making decisions about the location of the proton in this interactive system from spectroscopic data such as those of Polgár (1974) was pointed out by Shipton *et al.* (1975) and by Lowe (1976) and was discussed more generally by Dixon (1976). The difficulty of applying the frequently used Wegscheider principle of the supposed equivalence of protons and methyl groups (Wegscheider, 1902) to interactive systems such as that in the papain catalytic site has been discussed by Migliorini & Creighton (1986). Despite this difficulty, evidence that the interactive system of papain at neutral pH might exist to an appreciable and possibly to a substantial extent as $-S^-/-ImH^+$ ion-pair continues to accumulate both from kinetic studies with a variety of types of reactivity probe (see, e.g., Wallenfels & Eisele, 1968; Chaiken & Smith, 1969*a*,*b*; Jolley & Yankeelov, 1972; Stuchbury *et al.*, 1975; Shipton & Brocklehurst, 1977; Polgár & Halász, 1978; Polgár, 1979; Brocklehurst *et al.*, 1979*a*,*b*; Creighton *et al.*, 1980; Brocklehurst *et al.*, 1982; Migliorini & Creighton, 1986; Brocklehurst *et al.*, 1987) and from various types of spectroscopic study (see, e.g., Polgár, 1974; Creighton & Schamp, 1980; Johnson *et al.*, 1981; Lewis *et al.*, 1981). The other important structural feature of the catalytic site that is clearly revealed by the crystallographic data (Drenth *et al.*, 1976) is the 'oxyanion hole' (the side-chain NH_2 group of Gln-19 and the main-chain NH group of Cys-25), a hydrogen-bonding site towards which the carbonyl oxygen atom of the scissile amide group of a substrate is directed. The similarity in catalytic activity displayed by papain towards thionoester substrates and analogous ester substrates has led to the suggestion that the oxyanion hole is not operative in papain (Asbóth & Polgár, 1983; Polgár & Asbóth, 1986), but Storer & Carey (1985) argue convincingly that changes in the geometries of both enzyme and substrate during their interaction could well permit the oxyanion hole to accommodate the larger sulphur atom of thionoester substrates. The conformation of bound substrate in the active centre and the interactions involved in the binding, deduced by X-ray-crystallographic study of enzyme–inhibitor combinations (Drenth *et al.*, 1976), are supported to a considerable extent by the combined results of crystallographic and resonance Raman spectroscopic data involving a comparison of resonance Raman spectra of substrates of known conformation with resonance Raman spectra of dithioacyl derivatives of papain (Huber *et al.*, 1982; Storer *et al.*, 1983). The crystallographic studies of inhibitor binding have revealed movements both in the side chains of His-159 and Cys-25 and in the walls of the active-centre cleft in the region of the principal binding sites. The possibility of substantial rotation of the side chain of His-159 was revealed by the crystallographic studies performed by Drenth *et al.* (1976), and Baker & Drenth (1987) have emphasized that movement of the thiol group of Cys-25 and widening of the cleft during substrate or inhibitor binding are probably necessary because the essential catalytic residues have an almost zero solvent-accessible area in the native protein (Kamphuis *et al.*, 1985*a*).

In an attempt to detect and characterize changes in transition-state geometry in catalytic-site reactions of papain and other cysteine proteinases promoted by binding-site interactions, we recently suggested the use of unsymmetrical 2-pyridyl disulphides (R–S–S–2–Py) as reactivity probes (Brocklehurst *et al.*, 1987). A particularly striking change observed in the shape of the pH–second-order rate constant (k) profile (see also the Results and discussion section) consequent upon changing R from a simple alkyl group or 2-pyridyl to a group containing both an L-phenylalanyl side chain at P_2 and the P_1–P_2 amide bond suggested that one or both of these features might promote a change in transition-state geometry for the reaction of the catalytic-site thiol group. In the present paper we report pH-dependence studies showing that an analogous probe containing the P_1–P_2 amide bond but not the hydrophobic group at P_2 also appears to provide for a change in transition-state geometry in its reaction with papain, and kinetic isotope studies that suggest disruption of a hydrogen bond within the catalytic-site ion-pair $-S^- \cdots H\text{-}Im^+-$ when the P_1–P_2 amide bond is present in a substrate (*N*-methoxycarbonylglycine 4-nitrophenyl ester) or in a 2-pyridyl disulphide reactivity probe. Parts of this work have been reported in preliminary publications (Brocklehurst *et al.*, 1986; Quigley *et al.*, 1986).

MATERIALS AND METHODS

Materials

The purification of papain and the synthesis of (*a*) the minimal catalytic-site model, benzimidazol-2-ylmethanethiol, and (*b*) two disulphide reactivity probes: 2-(*N*′-acetyl-L-phenylalanylamino)ethyl 2′-pyridyl disulphide and 2-(acetamido)ethyl 2′-pyridyl disulphide have been described previously (see Brocklehurst *et al.*, 1987). Methoxycarbonylglycine 4-nitrophenyl ester was synthesized by the method of Werber & Shalitin (1973) and had m.p. 81 °C, as reported by Wharton & Szawelski (1982) [Werber & Shalitin (1973) give m.p. 80–83 °C]. 2,2′-Dipyridyl disulphide was obtained from Aldrich Chemical Co. and purified as described by Salih *et al.* (1987).

Ethyl 2-pyridyl disulphide was synthesized and purified by a method analogous to that used for the synthesis of methyl 2-pyridyl disulphide (Salih *et al.*, 1987), involving reaction of pyridine-2-thione (1.7 g, 15 mmol; Aldrich Chemical Co.) with ethyl ethanethiol sulphonate (1.54 g, 10 mmol). The chromatographically purified product (1.3 g, 76% yield based on the thiolsulphonate) was a pale-yellow oil, a sample of which produced the predicted yield of pyridine-2-thione consequent upon thiolysis with 2-mercaptoethanol at pH 7.0, deduced by spectral analysis at 343 nm ($\epsilon_{343} = 8080\ M^{-1} \cdot cm^{-1}$; Stuchbury *et al.*, 1975). The starting material, ethyl ethanethiolsulphonate, was synthesized by a procedure based on that reported by Smith *et al.* (1975) for the synthesis of methyl methanethiolsulphonate, involving oxidation of

the disulphide by H_2O_2. Diethyl disulphide (73 g, 0.6 mol; Aldrich Chemical Co.) was dissolved in acetic (ethanoic) acid (180 ml) in a three-necked flask fitted with dropping funnel, reflux condenser and thermometer, immersed in an ice/salt mixture. The solution was stirred vigorously by magnetic stirrer while H_2O_2 [170 ml of 30% (v/v), 1.2 mol] was added dropwise during a period of about 2 h so that the temperature of the reaction mixture did not exceed 10 °C. After the addition was complete, the reaction mixture was stirred for 24 h, during which time the temperature was allowed to rise to room temperature (approx. 22 °C) and the clear colourless solution became pale yellow. After this time no peroxides were detected in the reaction mixture when tested with starch paper. The bulk of the acetic acid was removed by rotary evaporation *in vacuo*, and the residual yellow oil was shaken with saturated aq. $NaHCO_3$ (100 ml) to neutralize residual acetic acid. The mixture was then extracted with chloroform (2 × 50 ml), and the chloroform layer was dried over anhydrous Na_2SO_4. The drying agent was removed by filtration, and the chloroform was removed from the filtrate by rotary evaporation. The residue, a clear yellow oil, was distilled to produce a colourless oil (23 g, 0.15 mol, 20% yield), b.p. 98 °C at 3.5 mmHg [Bodyrev *et al.* (1966) give b.p. 102 °C at 1–2 mmHg].

Kinetics

All reactions were studied at 25 °C and *I* 0.1. The reactions of the various pyridyl disulphide reactivity probes were carried out in Dionex stopped-flow equipment connected to a Tektronix 5103N oscilloscope and in some cases interfaced with either a Commodore 4032 microcomputer or a 380Z Research Machines microcomputer. Some kinetic runs in each set were recorded by photographing the oscilloscope screen, and conventional analysis of these records always provided values of rate constants in good agreement with those produced by the on-line microcomputers. Reactions with the 2-pyridyl disulphides were studied at 343 nm $\{\epsilon_{343} = 8.08 \times 10^3/(1 + K/[H^+])\ M^{-1} \cdot cm^{-1}$, where $pK = 9.8$ (Brocklehurst & Little, 1973; Stuchbury *et al.*, 1975)$\}$. The buffers were as described by Brocklehurst *et al.* (1987). Most reactions were carried out under pseudo-first-order conditions with [enzyme] or [low-M_r model mercaptan] 3–8 μM and [disulphide] 50–300 μM in the mixing chamber of the stopped-flow machine. Reactions of papain with 2-(*N'*-acetyl-L-phenylalanylamino)ethyl 2'-pyridyl disulphide were carried out under second-order conditions with [papain] 3–5 μM and [disulphide] 3–8 μM. For the reactions carried out under pseudo-first-order conditions, linear increase in the observed first-order rate constant with increase in [disulphide] confirmed that, under the conditions of concentration used both for the pH-dependence studies and for the kinetic isotope studies, the reactions obeyed overall second-order kinetics. Comparative kinetic studies in ^1H_2O and in ^2H_2O were carried out at equivalent pL 6.0 ($p^2H = pH + 0.4$; Glascoe & Long, 1960). The second-order rate constant (k) for reaction of all of the disulphide probes is relatively insensitive to change in pH at pH values around 6, so any small differences in pL would have only small effect on values of k. The papain-catalysed hydrolysis of methoxycarbonylglycine 4-nitrophenyl ester at pL 6.0 was studied at pL 6.0 with a Pye–Unicam SP. 1800 spectrophotometer by monitoring the increase in absorbance at 340 nm. Analysis of complete first-order progress curves for reactions with $[S]_0 \ll K_m$ together with the enzyme active-site concentration (determined by spectroscopic titration with 2,2'-dipyridyl disulphide; Brocklehurst & Little, 1973) provided values of the apparent second-order rate constant, $k_{cat.}/K_m$. For initial-rate studies, it is convenient to monitor product release from this and other 4-nitrophenyl ester substrates at 348 nm, which is an isosbestic point in the pH-dependent spectra of equilibrium mixtures of 4-nitrophenol and the 4-nitrophenolate ion ($\epsilon_{348} = 5.4 \times 10^3\ M^{-1} \cdot cm^{-1}$).

RESULTS AND DISCUSSION

Evidence for the importance of enzyme–substrate interactions in and near the S_2 subsite for the kinetic specificity of papain

Kinetic specificity arises from the mutual linking of substrate binding (characterized by the ES dissociation constant, K_s) and one or more of the subsequent steps in the catalytic process [characterized by the appropriate rate constant(s)]. This concept of utilization of the binding energy of the non-reacting parts of a specific substrate to increase reaction rate by realization of the binding energy in the transition state (Jencks, 1969, 1980) is central to current thinking about enzyme catalysis (Page, 1987; Wolfenden & Frick, 1987). In papain-catalysed hydrolysis the specificity is manifest in the process by which the thiol group of Cys-25 is acylated by adsorptively bound substrate. The central importance of the acylation process in this respect was clearly demonstrated by Lowe & Yuthavong (1971*a*) by steady-state kinetic analysis of the papain-catalysed hydrolysis of a number of ester and anilide substrates. Six of the substrates studied by Lowe & Yuthavong (1971*a*) that are structural analogues in important respects of the thiol-specific reactivity probes discussed below are compounds (I)–(VI). Their results nicely illustrate the extent to which the steady-state analysis was able to define the papain specificity and permitted the remaining uncertainties that seemed amenable to study by two-protonic-state reactivity probes to be identified. Thus the data for the three 4-nitrophenyl ester substrates [(I)–(III)], for which deacylation is rate-determining ($k_{cat.} = k_{+3}$) (at least at pH 6; see Ascenzi *et al.*, 1987), demonstrate the importance for the efficacy of the overall acylation process ($k_{cat.}/K_m$), at least for the benzoylglycine substrates, of the P_1–P_2 amide bond and the lack of importance of this bond for deacylation. The data for the three 4-nitroanilide substrates [(IV)–(VI)], for which acylation is either rate-determining ($k_{cat.} = k_{+2}$) or at least substantially slower than deacylation ($k_{+2} < k_{+3}$), demonstrate the importance of good S_2–P_2 contacts for high rates of acylation in substrates where the P_1–P_2 amide bond also exists. The steady-state kinetic data therefore demonstrate clearly that the kinetic specificity of papain is manifest in acylation and not in deacylation. They suggest also that *N*-acetyl-Phe-Gly- substrates provide for a more effective S_2–P_2 interaction than that provided by *N*-benzoyl-Gly- substrates, and that for the

(I) Ph–CO–NH–CH_2–CO–X (IV) CH_3–CO–Phe–NH–CH_2–CO–Y
(II) Ph–CO–CH_2–CH_2–CO–X (V) Ph–CO–NH–CH_2–CO–Y
(III) Ph–CH_2–CH_2–CH_2–CO–X (VI) CH_3–CO–NH–CH_2–CO–Y

X = –O– 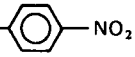 –NO_2 Y = –NH– 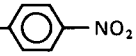 –NO_2

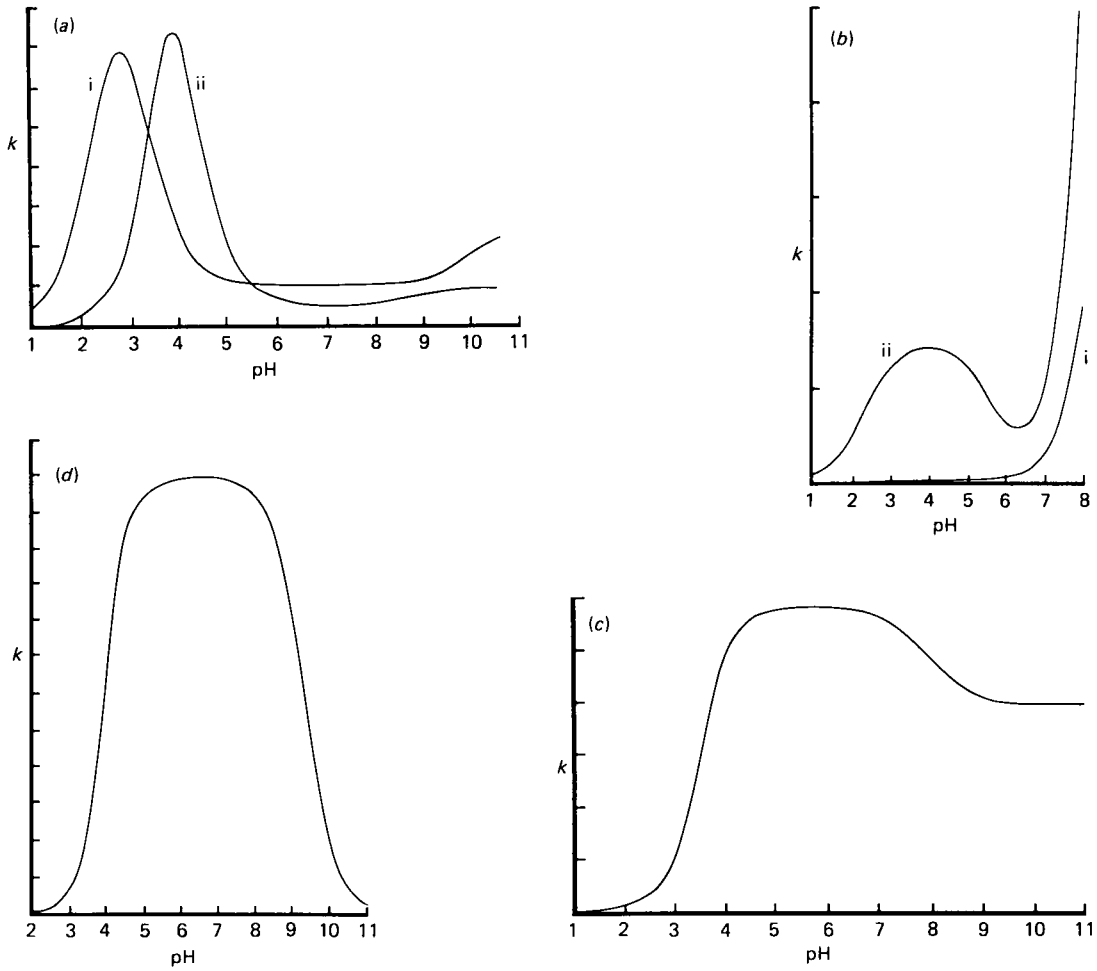

Fig. 1. Diagnostic value of disulphide reactivity probes containing a 2-mercaptopyridine leaving group for the characterization of cysteine proteinase catalytic-site interactive systems and of their modulation by binding interactions

The diagnostic value of these reactivity probes derives from the marked differences in the shapes of the pH–k profiles according to whether the 2-mercaptopyridine leaving group is activated by formal protonation at low pH or by association with a hydrogen-bond donor site in the enzyme. Typical values of k for various reactions are given in the text and in Figs. 2, 3 and 5. (*a*) Profiles typical of the reactions of cysteine proteinases such as (i) actinidin (EC 3.4.22.14) and (ii) papain with 2,2′-dipyridyl disulphide or with short-chain-alkyl 2-pyridyl disulphides. Activation of the probe is by formal protonation at low pH (pK_a approx. 2.5). The bell-shaped component occurs at higher pH for the papain reaction because of co-operative proton binding in this enzyme. (*b*) Profiles for reactions of the same type of probe reagents with (i) simple low-M_r mercaptans such as n-propanethiol and (ii) the minimal catalytic-site model benzimidazol-2-ylmethanethiol. (*c*) and (*d*) Profiles for reactions in which the 2-pyridyl disulphide probe binds to the enzyme in such a way that the 2-mercaptopyridine leaving group of the neutral probe molecule is activated by a hydrogen-bond donor in the enzyme, postulated for papain to be the imidazolium cation of His-159. The relative reactivities in the protonic states that predominate at pH values around 6 (the XH state) and at high pH (the X state) reflect the effectiveness of the activation process. Thus the activation is more effective in (*d*) than in (*c*), which may reflect a higher population of the transition-state geometry in which the appropriate hydrogen bond is made.

latter, at least, both carbonyl and amino components of the P_1–P_2 amide bond are necessary for the highest rates of acylation and hence of catalysis. X-ray-crystallographic data and model building (see, e.g., Lowe & Yuthavong, 1971*a*,*b*; Lowe, 1976; Drenth *et al.*, 1976; Baker & Drenth, 1987) suggest a structure for a papain–substrate adsorptive complex that permits rationalization of the steady-state kinetic data in terms of binding in the hydrophobic pocket of the S_2 subsite and interactions of P_1–P_2 amide bond across the active-centre cleft. The degree of interdependence of the S_2–P_2 interaction and the interaction of the components of the P_1–P_2 amide bond with the enzyme, and the change in this with change in substrate structure including possible further modulation by P_1–S_1 contacts, remain to be determined, as does the mechanism by which the binding energy is transduced to aid the acylation process.

Role of binding interactions in promoting change in transition-state geometry: detection by two-protonic-state reactivity probes

Clearly additional types of experiment are needed to determine the mechanisms by which the two types of binding interaction, i.e. S_2–P_2 and the interaction of the enzyme with the P_1–P_2 amide bond, bring about the rate enhancement in acylation detected by steady-state kinetic analysis. An important uncertainty was whether either or both types of interaction permit or promote detectable

rearrangement of catalytic-site and/or transition-state geometries in ways that would increase the rate of acylation. Perhaps the most obvious change in geometry involves the rearrangement of the mutual dispositions of the $-S^-$ and $-ImH^+$ components of the catalytic-site ion-pair. This might be expected to release or at least enhance the nucleophilic character of the thiolate anion and permit the imidazolium cation to play a role either as general acid catalyst by providing proton transfer to the leaving group in the transition state or as a stabilizing factor in a transition state before proton transfer.

We recently introduced an approach to the detection of such ligand-promoted rearrangements of catalytic-site geometry by using 2-pyridyl disulphides as thiol-specific two-protonic-state electrophilic reactivity probes (Brocklehurst *et al.*, 1987). The technique relies on (*a*) the activation of the electrophilic character of such disulphides either by formal protonation at low pH or by hydrogen-bonding with a suitable acidic side chain in the protein and (*b*) the very marked differences in plots of pH versus second-order rate constant (*k*) according to which of the activation mechanisms obtains and whether the attacking nucleophile is part of a low-pK_a interactive system or not. These marked changes in pH–*k* profile shape are illustrated in Fig. 1. Reaction of a low-pK_a interactive system such as those present in a number of cysteine proteinases, including papain, with a probe activated by formal protonation, and not by hydrogen-bonding with the catalytic-site imidazolium ion, results in a striking rate maximum in the pH region approx. 3–4 (Fig. 1*a*). This is true also for reaction of such a probe with benzimidazol-2-ylmethanethiol (VII) (Fig. 1*b*, curve ii), which contrasts markedly with the lack of a rate maximum in the corresponding reaction of a simple low-M_r mercaptan such as propanethiol (Fig. 1*b*, curve i). Compound (VII) may be regarded as a minimal low-M_r model for a cysteine proteinase catalytic site in that appreciable amounts of nucleophilic ion-pair exist in weakly acidic media.

One difference between the pH–*k* profile for the model (Fig. 1*b*, curve ii) and those for cysteine proteinases (Fig. 1*a*) is that the pK_a across which raising the pH produces nucleophilic character (ion-pair) is higher for the model (pK_a approx. 5.5) than for the enzymes (usually pK_a 3–4). When binding interactions between the non-reacting parts of the probe and the extended binding area of the enzyme result in the association of the catalytic-site imidazolium ion with the nitrogen atom of the 2-mercaptopyridine leaving group of the unprotonated probe, the reactivity of the protonic state that predominates at pH values around 6 ($\tilde{k}_{XH}$) would be expected to increase relative to that of the state at high pH ($\tilde{k}_X$), where the imidazolium ion has become deprotonated. One shape of such a pH–*k* profile (when $\tilde{k}_{XH} > \tilde{k}_X$) is shown in Fig. 1(*c*) and another (when $\tilde{k}_{XH} \gg \tilde{k}_X$ or when $\tilde{k}_X \simeq 0$) in Fig. 1(*d*).

The reaction of papain with 2-(*N*′-acetyl-L-phenylalanylamino)ethyl 2′-pyridyl disulphide (VIII), a reactivity probe containing both a potential occupant for the S_2 subsite (the phenylalanine side chain) and a P_1–P_2 amide bond is characterized by a pH–*k* profile of the type shown in Fig. 1(*d*) with a rate maximum at pH approx. 6 and $\tilde{k}_{XH} = 4.6 \times 10^6$ M$^{-1}\cdot$s^{-1} (Brocklehurst *et al.*, 1987). This contrasts markedly with the pH–*k* profiles for the reactions of papain with 2,2′-dipyridyl disulphide (Shipton & Brocklehurst, 1978) and with simple alkyl 2-pyridyl disulphides such as ethyl 2-pyridyl disulphide (see below). These profiles are of the type shown by curve ii in Fig. 1(*a*), with a rate minimum near to pH 6, with $\tilde{k}_{XH}$ approx. 1×10^3 M$^{-1}\cdot$s^{-1} for the former and approx. 5×10^3 M$^{-1}\cdot$s^{-1} for ethyl 2-pyridyl disulphide (see below), and a rate maximum at pH approx. 4.

In the present paper, the pH–*k* profile for the reaction of papain with 2-(acetamido)ethyl 2′-pyridyl disulphide (IX) is presented (Fig. 2) and compared with those for the reactions of (*a*) papain with ethyl 2-pyridyl disulphide (Fig. 3) and (*b*) the minimal catalytic-site model (VII) with the disulphide (IX) (Fig. 5). Compound (IX) may be considered to contain a P_1–P_2 amide bond but lacks a hydrophobic group that could bind in the S_2 subsite

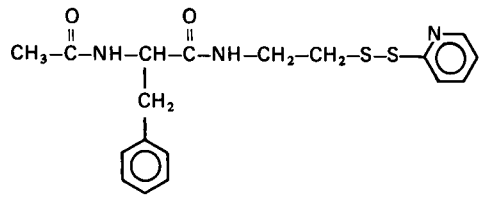

(VIII)

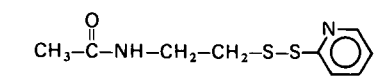

(IX)

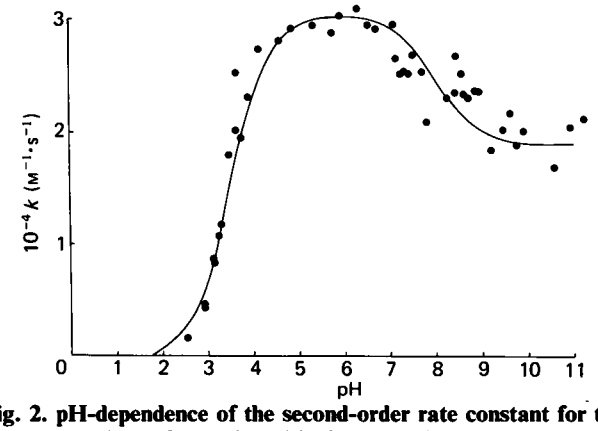

Fig. 2. pH-dependence of the second-order rate constant for the reaction of papain with 2-(acetamido)ethyl 2′-pyridyl disulphide (compound IX) are 25 °C and *I* 0.1 in aqueous buffers

The points are experimental and the line is theoretical for:

$$k = \tilde{k}_{+1}/[1+(10^{-pH})(10^{pK_I})+(10^{-pK_{II}})(10^{pH})] + \tilde{k}_{+2}/[1+(10^{-pH})(10^{pK_{II}})]$$

where $\tilde{k}_{+1} = 3.0 \times 10^4$ M$^{-1}\cdot$s^{-1}, $\tilde{k}_{+2} = 1.9 \times 10^4$ M$^{-1}\cdot$s^{-1}, pK_I = 3.5 and pK_{II} = 8.0.

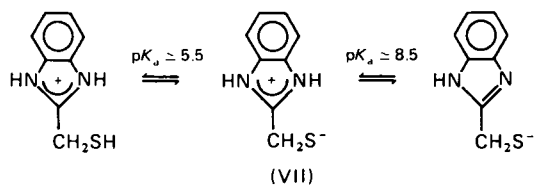

(VII)

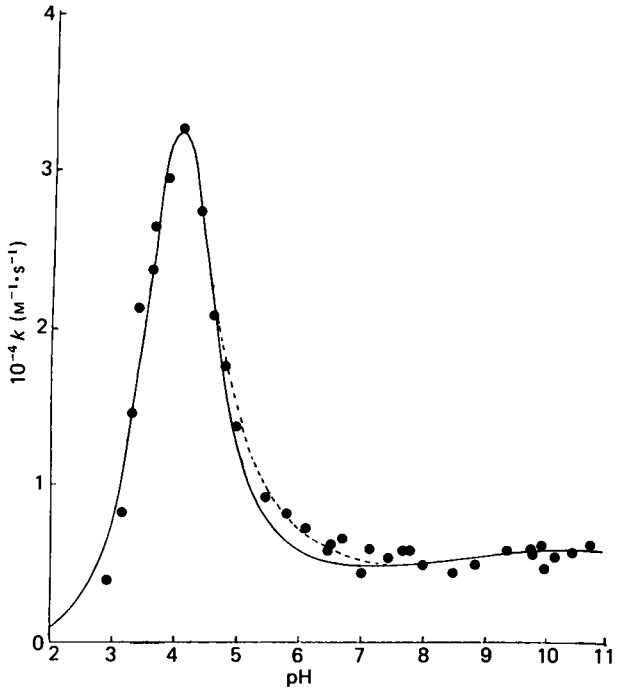

Fig. 3. pH-dependence of the second-order rate constant for the reaction of papain with ethyl 2-pyridyl disulphide at 25 °C and *I* 0.1 in aqueous buffers

The points are experimental and the continuous line is theoretical for:

$$k = \tilde{k}_{+1}/[1+(10^{-pH})(10^{pK_I})+(10^{-pK_{II}})(10^{pH})] + \tilde{k}_{+2}/[1+(10^{-pH})(10^{pK_{II}})+(10^{-pK_{III}})(10^{pH})] + \tilde{k}_{+3}/[1+(10^{-pH})(10^{pK_{III}})]$$

where $\tilde{k}_{+1} = 9.0\times10^4\ M^{-1}\cdot s^{-1}$, $\tilde{k}_{+2} = 5.0\times10^3\ M^{-1}\cdot s^{-1}$, $\tilde{k}_{+3} = 6.0\times10^3\ M^{-1}\cdot s^{-1}$ $pK_I = pK_{II} = 4.0$ and $pK_{III} = 8.8$. This line falls significantly below the data points in the pH region around 6. The broken line shows the effect on the theoretical line when an additional reactive protonic state with $\tilde{k} = 8.0\times10^3\ M^{-1}\cdot s^{-1}$ formed by protonic dissociation across $pK_a = 6.0$ is assumed to exist and $\tilde{k}_{+1} = 8.5\times10^4\ M^{-1}\cdot s^{-1}$ with the values of all other parameters unchanged. The bell-shaped component at low pH is characterized by two positively co-operative molecular pK_a values each of 4.0, a value substantially higher than that (2.9) of the pK_a of C_2H_5–S–S–2–PyH^+ determined by spectral analysis at 310 nm (see the text).

region. The pK_a of the conjugate acid of compound (IX) in which the pyridyl ring is protonated was determined to be 2.48 (at 25 °C and *I* 0.1) by the pH-dependent change in A_{310} (Fig. 4). The electronic spectra of disulphides containing the 2-mercaptopyridine group undergo large pH-dependent changes in u.v. absorption around 300 nm (see Salih *et al.*, 1987).

The striking difference between the pH–*k* profile (Fig. 2) for the reaction of papain with the disulphide containing the acetamido substituent (IX) and that (Fig. 3) for the reaction of papain with ethyl 2-pyridyl disulphide [(X), Table 1] is that only the former contains the rate maximum at pH 5–6, i.e. $\tilde{k}_{XH} > \tilde{k}_X$. Fig. 2 corresponds to the general profile shape shown in Fig. 1(*c*), and Fig. 3 corresponds to curve ii in Fig. 1(*a*). The profile for the reaction between the acetamido-containing probe and the minimal catalytic-site model (VII) (Fig. 5)

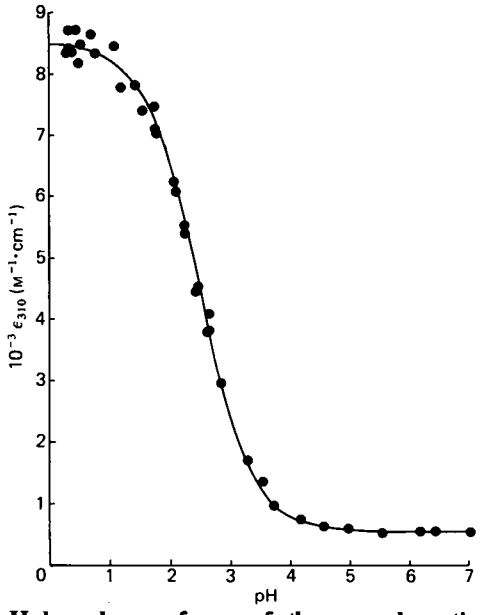

Fig. 4. pH-dependence of ε_{310} of the u.v. absorption by 2-(acetamido)ethyl 2′-pyridyl disulphide (compound IX) in aqueous media at 25 °C and *I* 0.1

The points were calculated from values of A_{310} of the pH-dependent spectra recorded by using a Cary 118C spectrophotometer (0–1*A* range) and the fitted line is theoretical for $pK_a = 2.48$.

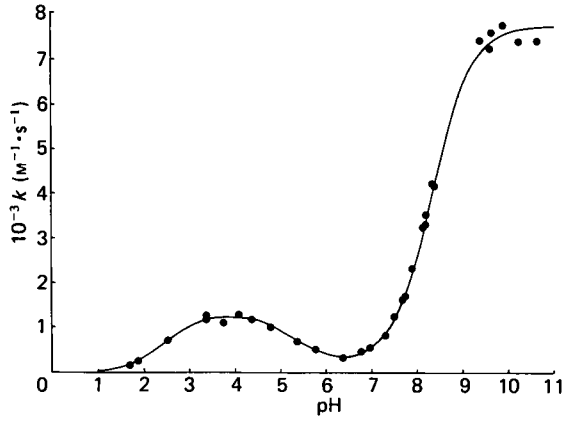

Fig. 5. pH-dependence of the second-order rate constant for the reaction of the minimal catalytic-site model benzimidazol-2-ylmethanethiol (compound VII) with 2-(acetamido)ethyl 2′-pyridyl disulphide (compound IX) at 25 °C and *I* 0.1 in aqueous buffers

The points are experimental and the line is theoretical for:

$$k = \tilde{k}_{+1}/[1+(10^{-pH})(10^{pK_I})+(10^{-pK_{II}})(10^{pH})] + \tilde{k}_{+2}/[1+(10^{-pH})(10^{pK_{II}})+(10^{-pK_{III}})(10^{pH})] + \tilde{k}_{+3}/[1+(10^{-pH})(10^{pK_{III}})]$$

where $\tilde{k}_{+1} = 1.3\times10^3\ M^{-1}\cdot s^{-1}$, $\tilde{k}_{+2} = 2.0\times10^2\ M^{-1}\cdot s^{-1}$, $\tilde{k}_{+3} = 7.7\times10^3\ M^{-1}\cdot s^{-1}$, $pK_I = 2.46$, $pK_{II} = 5.35$ and $pK_{III} = 8.33$; pK_I is in good agreement with the pK_a of the conjugate acid of the disulphide reagent determined to be 2.48 by spectral analysis (see Fig. 4).

contains a rate minimum at pH 6.5 (i.e. $\tilde{k}_{XH} < \tilde{k}_X$) and corresponds to the general profile shape of curve ii in Fig. 1(*b*). This is the shape predicted for reaction of the minimal catalytic-site model with a disulphide containing

Table 1. Variation in the reactivities of two protonic states of reactions of papain with change in probe structure

$\tilde{k}_{XH}$ and $\tilde{k}_X$ are pH-independent second-order rate constants characteristic of reaction in aqueous media at 25 °C and I 0.1, in protonic states that predominate at pH approx. 6 and at pH > 10 respectively.

Probe reagent	$\tilde{k}_{XH}$ ($M^{-1}\cdot s^{-1}$)	$\tilde{k}_X$ ($M^{-1}\cdot s^{-1}$)	$\tilde{k}_{XH}/\tilde{k}_X$	Reference
(XI) 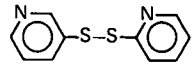	7.0×10^2	1.7×10^3	0.4	Salih *et al.* (1987)
(XII) 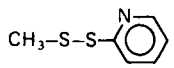	2.2×10^4	3.9×10^4	0.6	Salih *et al.* (1987)
(X) 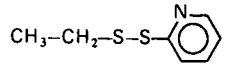	5.0×10^3	6.0×10^3	0.8	Present work
(IX) 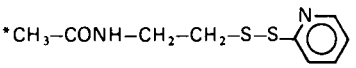	3.0×10^4	1.9×10^4	1.6	Present work
(VIII) 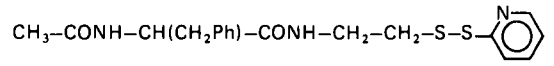	4.6×10^6	$\leqslant\sim 1\times10^6$	$\geqslant\sim 5$	Brocklehurst *et al.* (1987)

* The corresponding values of the parameters for the reaction of this disulphide with the minimum catalytic-site model, benzimidazol-2-ylmethanethiol, are $\tilde{k}_{XH} = 2.0\times10^2$ $M^{-1}\cdot s^{-1}$, $\tilde{k}_X = 7.7\times10^3$ $M^{-1}\cdot s^{-1}$ and $\tilde{k}_{XH}/\tilde{k}_X = 0.03$.

a 2-mercaptopyridine leaving group; pK_I (= 2.46) corresponds to the pK_a of the protonated pyridyl ring (2.48; see Fig. 4) and pK_{II} and pK_{III} correspond to the first and second pK_a values respectively of benzimidazol-2-ylmethanethiol (VIII). Chemical experience suggests that reaction in the protonic state that predominates around the pH optimum of 3–4 involves protonated 2-pyridyl disulphide and the zwitterionic form of the mercaptan, i.e. the reactive ionic forms are those of the minor protonic state with 'crossed-over' pK_a values [see Malthouse & Brocklehurst (1976) and Brocklehurst & Malthouse (1980) for a discussion of minor protonic states]. Thus the reactivity characteristics of 2-(acetamido)ethyl 2′-pyridyl disulphide (IX) towards the low-M_r model are quite normal, and its abnormal reactivity characteristics towards papain must derive, therefore, from binding interactions between enzyme and reactivity probe. The comparison of reactivities in the XH state (predominating at pH 5–7) and in the X state (predominating at high pH) for papain–probe reactions presented in Table 1 serves to emphasize that a rate maximum at pH approx. 6 ($\tilde{k}_{XH} > \tilde{k}_X$) is produced when the probe reagent contains a P_1–P_2 amide bond and that this is further accentuated (i.e. $\tilde{k}_{XH}/\tilde{k}_X$ is increased) when, in addition, a hydrophobic substituent is present at P_2. Presumably the interaction of the S_2 subsite with the hydrophobic substituent at P_2 results in an increase in the population of transition states in which the pyridyl nitrogen atom successfully encounters the imidazolium side chain of the catalytic-site histidine residue of papain as in transition state (XIII). This transition state depicts nucleophilic attack by thiolate anion with stabilization due to hydrogen-binding-cum-electrostatic interaction provided by the imidazolium cation. The reasons for preferring this transition state to one in which proton transfer from $-ImH^+$ occurs synchronously with

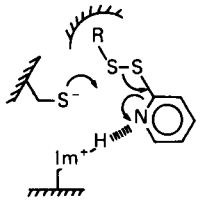

(XIII)

nucleophilic attack are given below in the discussion on kinetic solvent isotope effects. A rate maximum at pH approx. 6 is characteristic also of plots of pH versus $k_{cat.}/K_m$ ($= k_{+2}/K_s$, the overall second-order rate constant for acylation) for papain-catalysed hydrolysis (see, e.g., Lowe & Yuthavong, 1971*b*; Mole & Horton, 1973; Mackenzie *et al.*, 1985; Storer & Carey, 1985), and it seems possible that the P_1–P_2 amide bond may play a similar role in catalysis to that deduced for the probe reactions, i.e. a role in controlling, through specific binding interactions, the encounter of the catalytic-site imidazolium ion with the leaving group of the substrate.

Kinetic solvent ^2H-isotope effects on the reactions of the papain thiol group with various electrophilic reagents

The results (see Table 1) from studies on the pH-dependence of the rates of reaction of the papain thiol group with the various 2-pyridyl disulphides, discussed above, suggested that the introduction of a P_1–P_2 amide bond into the electrophilic probe molecule allows a new transition state geometry involving both nucleophilic attack by enzyme thiolate anion and encounter of the pyridyl nitrogen atom with the enzyme imidazolium cation (XIII) and that this pathway might be further promoted by good P_2–S_2 contacts (see Fig. 6*a*).

Table 2. Variation in the overall kinetic solvent ^2H-isotope effect at 25 °C for reactions of papain with change in the structure of the substrate or thiol-specific reactivity probe

For the reactions of the disulphide probes, k is the second-order rate constant at pL 6.0; for the reactions of the alkylating agents, k is $\tilde{k}_{XH}$, which is similar to k at pL 6; for the catalysed-hydrolysis of methoxylcarbonylglycine 4-nitrophenyl ester (XIV), k is $k_{cat.}/K_m$ at pL 6.0; for the catalysed hydrolyses of the other substrates, k is $k_{cat.(XH)}/K_{m(XH)}$, which is similar to $k_{cat.}/K_m$ at pL 6; in all cases values of $k_{cat.}/K_m$ are sufficiently small to provide a good approximation to k_{+2}/K_s, the second-order rate constant for the acylation of papain by substrate [Brocklehurst (1979); eqn. (2) in that paper should read: $k = k_{+1}k_{+2}/(k_{-1}+k_{+2})$].

	Substrate or probe reagent	k^{1H_2O}/k^{2H_2O}	Reference
(XI)	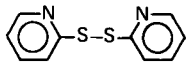	0.96±0.03	Present work
(IX)	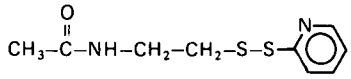	0.75±0.03	Present work
(VIII)	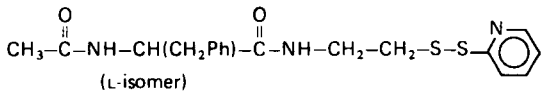 (L-isomer)	0.61±0.01	Present work
(XIV)	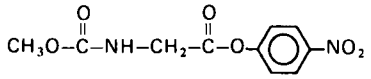	0.67	Present work
(XV)	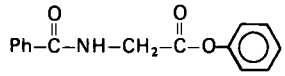	0.63	Polgár & Halász (1978); Polgár (1979)
(XVI)	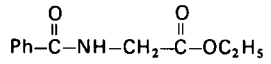	1.07	Polgár & Halász (1978); Polgár (1979)
(XVII)	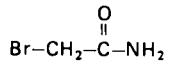	0.74	Polgár & Halász (1978); Polgár (1979)
(XVIII)	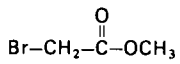	1.03	Polgár & Halász (1978); Polgár (1979)
(XIX)	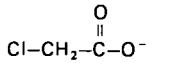	0.75±0.07	Wandinger & Creighton (1980)
(XX)	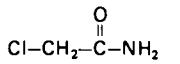	1.0	Wandinger & Creighton (1980)

In an attempt to obtain further support for this postulated consequence of enzyme–ligand interaction in the S_1–S_2 intersubsite region of papain, the solvent kinetic ^2H-isotope effects on the enzyme–probe reactions were determined at pL 6.0, where the hydronic state containing the neutral probe reagent and the ion-pair form of the catalytic site (and/or its neutral SH/Im tautomer) predominates. The value of the kinetic solvent ^2H-isotope effect for this purpose had been suggested by the earlier work of Polgár (1979) and of Creighton *et al.* (1980) on the reactions of papain with various alkylating agents and substrates. Some of their data are presented with the results of the present work in Table 2 and are considered below, following discussion of our own data.

With regard to the reactions of the ion-pair state of papain with the three 2-pyridyl disulphide probes (VIII), (IX) and (XI), the trend in the kinetic solvent ^2H-isotope effects seems to be clear and correlates well with trends identified in the pH-dependence studies. Thus: (i) reaction with 2,2′-dipyridyl disulphide (XI), which does not contain a P_1–P_2 amide bond, displays no isotope effect (i.e. $k^{1H_2O}/k^{2H_2O} = 1.0$) and the pH–$k$ profile is characterized by a rate minimum at pH values near to 6; (ii) reaction with 2-(acetamido)ethyl 2′-pyridyl disulphide (IX), which contains a P_1–P_2 amide bond, displays an inverse kinetic solvent isotope effect, i.e. $k^{1H_2O}/k^{2H_2O} < 1.0$ ($k^{1H_2O}/k^{2H_2O} = 0.75$) and the pH–$k$ profile is characterized by a rate maximum at pH values near to 6; (iii) reaction with 2-(*N*′-acetyl-L-phenylalanylamino)-ethyl 2′-pyridyl disulphide (VIII), which contains both a P_1–P_2 amide bond and a potential occupant for the S_2 subsite, displays an even greater inverse kinetic solvent isotope effect, i.e. an even smaller value of k^{1H_2O}/k^{2H_2O} (= 0.6) and the rate maximum at pH values near to 6 is more fully developed (cf. Figs. 1*d* and 2). These correlations suggest that, whatever binding effects of papain and probe reagent are responsible for the

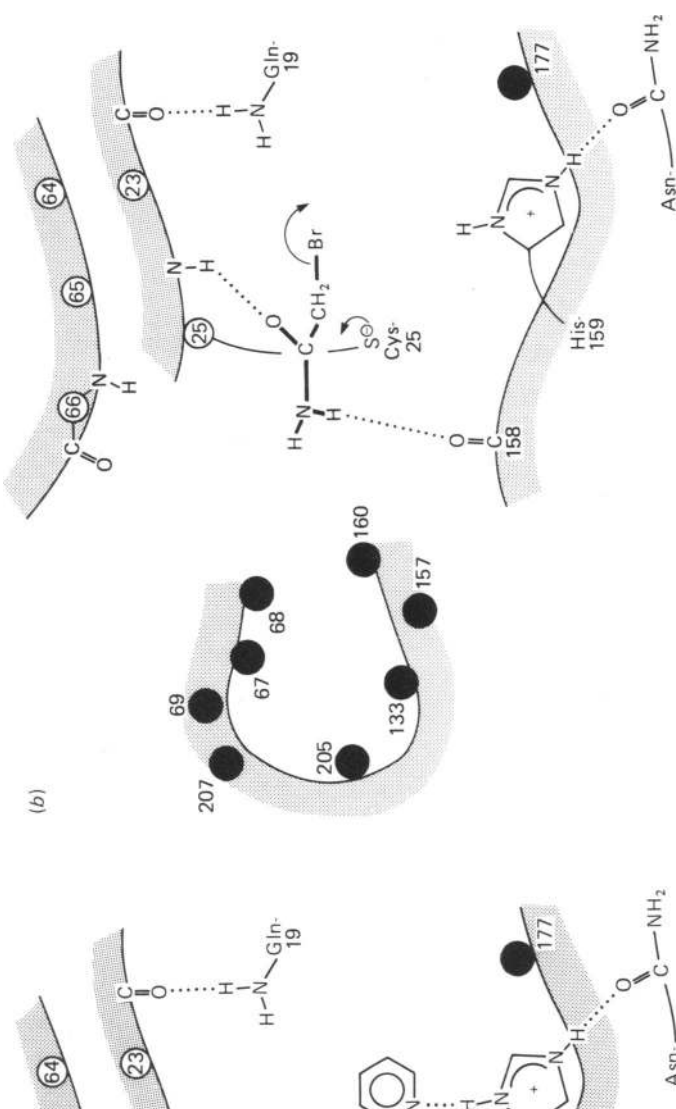

Fig. 6. Schematic drawings showing possible interactions between papain and two electrophilic reactivity probes postulated to contribute to the kinetic characteristics of the reactions

(*a*) Reaction of papain with 2-(*N*'-acetyl-L-phenylalanylamino)ethyl 2'-pyridyl disulphide: the interaction of the P_1–P_2 amide bond of the probe molecule across the active-centre cleft by hydrogen-bonding with the backbone carbonyl oxygen atom of Asp-158 and with the backbone N–H of Gly-66, augmented by the binding of the phenyalanine side chain in the hydrophobic pocket of the S_2 subsite, appears to be responsible for an adsorptive complex and transition-state geometry in which $-S^-/-ImH^+$ ion-pair has been disrupted and nucleophilic attack by $-S^-$ of Cys-25 is assisted by association of the pyridyl nitrogen atom with the imidazolium ion of His-159. (*b*) Reaction of papain with bromoacetamide: the probe reagent is shown in hydrogen-bonding interaction with the backbone carbonyl oxygen atom of Asp-158 as suggested by Polgár (1979); another hydrogen bond with the backbone N–H of Cys-25, part of the postulated oxyanion hole, might be an additional possibility. This Figure was adapted from the schematic drawing of a papain–substrate complex that was kindly supplied by Professor Jan Drenth and Dr. Ted Baker. The structural features of the ES complex were deduced from crystallographic studies on enzyme–inhibitor combinations (Drenth *et al.*, 1976). In the enzyme–inhibitor combination, the terminal methylene group of an inhibitor such as *N*-benzyloxycarbonyl-Phe-Ala-CH_2Cl is attached to S_γ of Cys-25, and the carbonyl oxygen atom adjacent to it (i.e. of P_1 C=O, which corresponds to the C=O of the scissile peptide bond of a substrate) is directed towards two NH groups. These are the main-chain NH group of residue 25, which is at the *N*-terminus of α-helix 24–42, and an NH group of the amide side chain of Gln-19. The peptide between P_1 and P_2 lies near the extended piece of chain comprising residues 65–67 of the wall of the active-centre cleft such that the P_2 NH and C=O groups can hydrogen-bond with the C=O and NH groups respectively of Gly-66 and the P_1 NH group is directed towards the C=O group of residue 158 on the opposite wall of the cleft. The side chain of residue P_2 (Phe) is accommodated so that $C_{(\beta)}$ lies between the side chains of Pro-68 and Ala-160, and beyond it the phenyl ring is adjacent to the side chains of Val-133 and Val-157, which with Tyr-67, Trp-69 and Phe-207 form the hydrophobic binding pocket. No attempt has been made to depict changes in enzyme conformation in the catalytic-site region that might result from the binding interactions, particularly those shown in (*a*).

differential development of high rates of reaction at pH values around 6, they result also in the progressive development of an inverse ^{2}H-kinetic solvent isotope effect. Inverse isotope effects of the magnitude observed could arise from the breaking of a hydrogen bond between the components of the catalytic-site ion-pair. This would be consistent with the range of fractionation factors ϕ for hydrogen-bonded systems discussed by Kreevoy & Liang (1980). The inverse isotope effects here reported probably have their origin in a combination of ground-state and medium effects. One of the major conclusions of the isotope work is that a proton is not in the process of transfer in the transition state. Proton transfer in the transition state, with $\phi \ll 1$, would almost certainly result in a normal solvent kinetic isotope effect. Thus the transition state responsible for the rate maxima at pH 6 (Figs. 1*c*, 1*d* and 2) is probably like that depicted in transition state (XIII), in which the imidazolium cation provides stabilization via a 'loose' hydrogen bond with $\phi \simeq 1.0$, with post-transition state proton transfer. This conclusion is supported by the work of Gilbert & Jencks (1977) on the mechanisms of the acid-catalysed additions of mercaptans to carbonyl groups

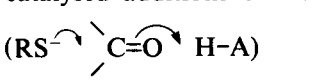

As the addition product becomes more stable the degree of proton transfer in the transition state decreases from concerted to strongly hydrogen-bonding to weakly hydrogen-bonding, which provides a stepwise mechanism of nucleophilic attack followed by proton transfer. The reactions of papain with the disulphides provide a very stable (isolable) addition product and thus a stepwise mechanism would be predicted.

The data shown in Table 2 for the reactions of papain with the three alkylating agents (XVII)—(XIX) may be interpreted to support the view deduced above from the data for the 2-pyridyl disulphide probes that an inverse isotope effect is connected in some way with the disruption of the intimate $-S^-/-ImH^+$ ion-pair and the formation of a new interaction involving $-ImH^+$ and the reagent. The –N–H group of bromoacetamide might hydrogen-bond with the backbone carbonyl oxygen atom of Asp-158 (one of the intersubsite interactions envisaged for a P_1–P_2 amide bond) as suggested by Polgár (1979), although since this reagent is a 'reverse amide' the other part of the interaction of a P_1–P_2 amide bond ($>C=O$ hydrogen-bonding with backbone –N–H of Gly-66) is not possible (Fig. 6*b*). This may be the reason for the exhibition of an inverse isotope effect without the additional characteristic of $\tilde{k}_{XH} > \tilde{k}_X$, i.e. a bell-shaped pH–*k* profile. The lack of a kinetic isotope effect for the reaction of papain with methyl bromoacetate (VIII) (Polgár, 1979) is in accord with the absence of an interaction of an –N–H bond in the reagent with the enzyme. The fact that the reaction of papain with chloroacetate (IX) also displays an inverse isotope effect, of similar magnitude to that displayed by the reaction of bromoacetamide, may be accounted for again by interruption of the $-S^-/-ImH^+$ ion-pair, but in this case by a direct electrostatic interaction of the $-ImH^+$ component with the carboxylate anion of the reagent (XXI), rather than by an indirect effect involving interaction in the S_1–S_2 intersubsite region of the enzyme. This is the type of interaction favoured by Creighton *et al.* (1980) not only for the reaction of chloroacetate

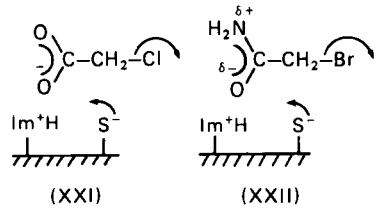

(XXI) (XXII)

(XXI) but also for the reaction of bromoacetamide (XXII). The latter contrasts with the interpretation of the kinetic isotope effect for this reagent suggested by Polgár (1979) and discussed above (see Fig. 6*b*).

Although the kinetic study of the reaction of papain with bromoacetamide appears to have been restricted to pH values below 6 (see, e.g., Polgár & Halász, 1978), analogy with reactions of papain with other neutral alkylating agents (see, e.g., Polgár, 1973) suggests the probability of a double-sigmoid pH–*k* profile for this reaction. If this is the case, the suggestion by Creighton *et al.* (1980) of a significant interaction between reagent and $-ImH^+$ in transition state (XXII) as well as in transition state (XXI) would not seem readily able to account for a bell-shaped pH–*k* profile only in the case of the former if the population of the transition state (XXII) is comparable with that of the transition state (XXI).

One other noteworthy feature of the data in Table 2 is the contrast between the inverse kinetic isotope effect for the bromoacetamide reaction and the lack of a kinetic isotope effect for the chloroacetamide reaction. Wandinger & Creighton (1980) have suggested that the reason for this lack of uniformity of isotope effects with different alkylating agents may derive from the existence of intermediate adsorptive complexes between enzyme and reagent before covalency change. This could lead to compensating isotope effects between different steps of the mechanism.

We have previously pointed out the value of taking account of the possibility that reactions of enzyme nucleophiles with site-specific reagents that are not formally substrate analogues may well proceed through the intermediacy of adsorptive complexes, albeit characterized by rather large dissociation constants, in connection with pH–rate studies (Brocklehurst & Dixon, 1976, 1977; Brocklehurst, 1979). This view is further emphasized by the discussion by Wandinger & Creighton (1980) on isotope effects, which shows that certain interpretations may not become apparent if the possibility of formation of adsorptive complex involving enzyme and small molecules is neglected.

Interpretation of isotope effects for the acylation step of catalysis is necessarily more complex, particularly in view of the multistep nature of the covalency changes. Polgár (1979) had noted a substantial inverse kinetic isotope effect for substrates containing hydrophobic leaving groups and both the P_1–P_2 amide bond and a hydrophobic group that might bind near to the mouth of the S_2 subsite. In the present work we have added a little to this by demonstrating a similar inverse kinetic isotope effect for the acylation of papain by *N*-methoxycarbonylglycine 4-nitrophenyl ester, a substrate that lacks a hydrophobic occupant for the S_2 subsite but that contains the other two features of the ester substrates used by Polgár (1979). The inverse kinetic isotope effect is lost when the aromatic leaving group is replaced by an

aliphatic leaving group in ester substrates, but is retained when amide substrates such as *N*-benzoyl-Arg-NH_2, *N*-benzoyl-Cit-NH_2 or *N*-benzyloxycarbonyl-Phe-Gly-NH_2 are used (Polgár, 1979). In the case of the amide substrates, Polgár (1979) suggests that competition between the –N–H of the leaving group and the –N–H of the P_1–P_2 amide bond for the backbone carbonyl oxygen atom of Asp-158 (see also Asbóth & Polgár, 1977*a*,*b*) may contribute to the inverse kinetic isotope effect.

Concluding remarks

The coupling of binding-site interactions with catalytic-site chemistry appears to be an important part of the recognition process in reactions of papain. In particular, the hydrogen-bonding of an –N–H group of a ligand in the S_1–S_2 intersubsite region of the enzyme, probably to the backbone carbonyl oxygen atom of Asp-158, appears to allow a transition-state geometry involving both $-S^-$ and $-ImH^+$ components of the catalytic site. The development of a new transition-state geometry involving a new mutual disposition of ion-pair components is detected particularly clearly by 2-pyridyl disulphide reactivity probes, because of the sensitivity of the thiol–disulphide interchange in 2-mercaptopyridine systems to association of the pyridyl nitrogen atom with the catalytic-site imidazolium cation. The correlation of the shift in the rate maximum from pH 4 to pH 6 with the development of an inverse kinetic solvent isotope effect as the ligand structure is varied suggests that the binding of the –N–H of the ligand to the backbone carbonyl oxygen atom of Asp-158 may promote the breaking of a hydrogen bond within the catalytic-site ion-pair. If this proves to be the case, the specific binding of a substrate in the S_1–S_2 intersubsite region of papain may be part of the process whereby binding energy is used in assisting the catalytic act by permitting the correct transition-state geometry for acylation of the enzyme nucleophile to be achieved.

We thank the Science and Engineering Research Council for projects grants, for a Research Studentship for K. Q. and for an Earmarked Research Studentship for D. K., Miss Betty Wilkie and Miss Jackie Scott for valuable technical assistance, Mr. Simon M. Brocklehurst for writing the computer program used to evaluate multiprotonic-state pH–*k* profiles, Miss Joy Smith for the rapid production of the typescript, and Professor Jan Drenth and Dr. Ted Baker for supplying a copy of a schematic drawing of a papain–substrate complex that was used to construct Fig. 6.

REFERENCES

Asbóth, B. & Polgár, L. (1977*a*) Acta Biochim. Biophys. Acad. Sci. Hung. **12**, 223–230

Asbóth, B. & Polgár, L. (1977*b*) Acta Biochim. Biophys. Acad. Sci. Hung. **12**, 329–333

Asbóth, B. & Polgár, L. (1983) Biochemistry **22**, 117–122

Ascenzi, P., Aducci, P., Torroni, A., Amiconi, G., Ballio, A., Menegatti, E. & Guarneri, M. (1987) Biochim. Biophys. Acta **912**, 203–210

Baker, E. N. & Drenth, J. (1987) in Biological Macromolecules and Assemblies (Jurnak, F. & McPherson, A., eds.), vol. 3, pp. 313–368, John Wiley and Sons, New York

Berger, A. & Schechter, I. (1970) Philos. Trans. R. Soc. London B **257**, 249–264

Bodyrev, V. G., Slesarchuk, L. P., Gatala, E. E., Trofimova, T. A. & Vasenko, E. N. (1966) J. Org. Chem. USSR (Engl. Transl.) **2**, 91–97

Brocklehurst, K. (1974) Tetrahedron **30**, 2397–2407

Brocklehurst, K. (1979) Biochem. J. **181**, 775–778

Brocklehurst, K. (1982) Methods Enzymol. **87C**, 427–469

Brocklehurst, K. (1986) in Cysteine Proteinases and their Inhibitors (Turk, V., ed.), pp. 307–325, Walter de Gruyter, Berlin

Brocklehurst, K. (1987) in Enzyme Mechanisms (Page, M. I. & Williams, A., eds.), pp. 140–158, Royal Society of Chemistry, London

Brocklehurst, K. & Dixon, H. B. F. (1976) Biochem. J. **155**, 61–70

Brocklehurst, K. & Dixon, H. B. F. (1977) Biochem. J. **167**, 859–862

Brocklehurst, K. & Little, G. (1973) Biochem. J. **133**, 67–80

Brocklehurst, K. & Malthouse, J. P. G. (1980) Biochem. J. **191**, 707–718

Brocklehurst, K., Malthouse, J. P. G. & Shipton, M. (1979*a*) Biochem. J. **183**, 223–231

Brocklehurst, K., Herbert, J. A. L., Norris, R. & Suschitzky, H. (1979*b*) Biochem. J. **183**, 369–373

Brocklehurst, K., Baines, B. S. & Kierstan, M. P. J. (1981) Top. Enzyme Ferment. Biotechnol. **5**, 262–335

Brocklehurst, K., Mushiri, S. M., Patel, G. & Willenbrock, F. (1982) Biochem. J. **201**, 101–104

Brocklehurst, K., Kowlessur, D., Patel, G., Templeton, W., Thomas, E. & Willenbrock, F. (1986) Biochem. Soc. Trans. **14**, 1225–1226

Brocklehurst, K., Kowlessur, D., O'Driscoll, M., Patel, G., Quenby, S., Salih, E., Templeton, W., Thomas, E. W. & Willenbrock, F. (1987) Biochem. J. **244**, 173–181

Brocklehurst, K., Willenbrock, F. & Salih, E. (1988) New Compr. Biochem. **16**, 39–158

Chaiken, I. M. & Smith, E. L. (1969*a*) J. Biol. Chem. **244**, 5087–5094

Chaiken, I. M. & Smith, E. L. (1969*b*) J. Biol. Chem. **244**, 5095–5099

Creighton, D. J. & Schamp, D. J. (1980) FEBS Lett. **110**, 313–318

Creighton, D. J., Gessouroun, M. S. & Heapes, J. M. (1980) FEBS Lett. **110**, 319–322

Dixon, H. B. F. (1976) Biochem. J. **153**, 627–629

Drenth, J., Kalk, K. H. & Swen, H. M. (1976) Biochemistry **15**, 3731–3738

Fruton, J. S. (1977) Proc. Am. Philos. Soc. **121**, 309–315

Fruton, J. S. (1982) Adv. Enzymol. Relat. Areas Mol. Biol. **53**, 239–306

Gilbert, H. F. & Jencks, W. P. (1977) J. Am. Chem. Soc. **99**, 7931–7947

Glascoe, P. K. & Long, F. A. (1960) J. Phys. Chem. **64**, 188–191

Huber, C. P., Ozaki, Y., Pliura, D. H., Storer, A. C. & Carey, P. R. (1982) Biochemistry **21**, 3109–3115

Jencks, W. P. (1969) Catalysis in Chemistry and Enzymology, pp. 282–320, McGraw-Hill, New York

Jencks, W. P. (1980) Adv. Enzymol. Relat. Areas Mol. Biol. **51**, 75–106

Johnson, F. A., Lewis, S. D. & Shafer, J. A. (1981) Biochemistry **20**, 44–48

Jolley, C. J. & Yankeelov, J. A. (1972) Biochemistry **11**, 164–169

Kamphuis, I. G., Kalk, K. H., Swarte, M. B. & Drenth, J. (1984) J. Mol. Biol. **179**, 233–256

Kamphuis, I. G., Kalk, K. H., Swarte, M. B. A. & Drenth, J. (1985*a*) J. Mol. Biol. **179**, 233–256

Kamphuis, I. G., Drenth, J. & Baker, E. N. (1985*b*) J. Mol. Biol. **182**, 317–329

Kreevoy, M. M. & Liang, T. (1980) J. Am. Chem. Soc. **102**, 3315–3322

Lewis, S. D., Johnson, F. A. & Shafer, J. A. (1981) Biochemistry **20**, 48–51

Lowe, G. (1976) Tetrahedron **32**, 291–302
Lowe, G. & Yuthavong, Y. (1971*a*) Biochem. J. **124**, 107–115
Lowe, G. & Yuthavong, Y. (1971*b*) Biochem. J. **124**, 117–122
Mackenzie, N. E., Malthouse, J. P. G. & Scott, A. I. (1985) Biochem. J. **226**, 601–606
Malthouse, J. P. G. & Brocklehurst, K. (1976) Biochem. J. **159**, 221–234
Migliorini, M. & Creighton, D. J. (1986) Eur. J. Biochem. **156**, 189–192
Mole, J. E. & Horton, H. R. (1973) Biochemistry **12**, 816–822
Page, M. I. (1987) in Enzyme Mechanisms (Page, M. I. & Williams, A., eds.), pp. 1–13, Royal Society of Chemistry, London
Polgár, L. (1973) Eur. J. Biochem. **33**, 104–109
Polgár, L. (1974) FEBS Lett. **47**, 15–18
Polgár, L. (1979) Eur. J. Biochem. **98**, 369–374
Polgár, L. & Asbóth, B. (1986) J. Theor. Biol. **121**, 323–326
Polgár, L. & Halász, P. (1978) Eur. J. Biochem. **88**, 513–521
Polgár, L. & Halász, P. (1982) Biochem. J. **207**, 1–10
Quigley, K., Szawelski, R. J. & Wharton, C. W. (1986) Biochem. Soc. Trans. **14**, 1287–1288
Salih, E., Malthouse, J. P. G., Kowlessur, D., Jarvis, M., O'Driscoll, M. & Brocklehurst, K. (1987) Biochem. J. **247**, 181–193
Schechter, I. & Berger, A. (1967) Biochem. Biophys. Res. Commun. **27**, 157–162
Schechter, I. & Berger, A. (1968) Biochem. Biophys. Res. Commun. **32**, 898–902
Shipton, M. & Brocklehurst, K. (1977) Biochem. J. **167**, 799–810
Shipton, M. & Brocklehurst, K. (1978) Biochem. J. **171**, 385–401
Shipton, M., Kierstan, M. P. J., Malthouse, J. P. G., Stuchbury, T. & Brocklehurst, K. (1975) FEBS Lett. **50**, 365–368
Smith, D. J., Maggio, E. T. & Kenyon, G. L. (1975) Biochemistry **14**, 766–771
Storer, A. C. & Carey, P. R. (1985) Biochemistry **24**, 6808–6818
Storer, A. C., Lee, H. & Carey, P. R. (1983) Biochemistry **22**, 4789–4796
Stuchbury, T., Shipton, M., Norris, R., Malthouse, J. P. G., Brocklehurst, K., Herbert, J. A. L. & Suschitzky, H. (1975) Biochem. J. **151**, 417–432
Wallenfels, K. & Eisele, B. (1968) Eur. J. Biochem. **3**, 267–275
Wandinger, A. & Creighton, D. J. (1980) FEBS Lett. **116**, 116–122
Wegscheider, R. (1902) Monatsh. Chem. **23**, 287–316
Werber, M. M. & Shalitin, Y. (1973) Bioorg. Chem. **2**, 202–220
Wharton, C. W. & Szawelski, R. J. (1982) Biochem. J. **203**, 351–360
Wolfenden, R. & Frick, L. (1987) in Enzyme Mechanisms (Page, M. I. & Williams, A., eds.), pp. 97–122, Royal Society of Chemistry, London
Wolthers, B. G., Drenth, J., Jansonius, J. N., Koekoek, R. & Swen, H. M. (1970) Proc. Int. Symp. Structure–Function Relationships of Proteolytic Enzymes (Desnuelle, P., Neurath, H. & Ottesen, M., eds.), pp. 272–288, Munksgaard, Copenhagen

Received 13 July 1987/11 September 1987; accepted 12 November 1987